Tuning the phase separation in $La_{0.325}Pr_{0.3}Ca_{0.375}MnO_3$ using the electric double-layer field effect*

Cui Li-Min(崔丽敏), Li Jie(李 洁), Zhang Yu(张 玉), Zhao Lu(赵 璐), Deng Hui(邓 辉), Huang Ke-Qiang(黄克强), Li He-Kang(李贺康), and Zheng Dong-Ning(郑东宁)†

Beijing National Laboratory for Condensed Matter Physics, Institute of Physics, Chinese Academy of Sciences, Beijing 100190, *China*

(Received 8 April 2013; revised manuscript received 16 May 2014; published online 16 July 2014)

Electric double-layer field effect experiments were performed on ultrathin films of $La_{0.325}Pr_{0.3}Ca_{0.375}MnO_3$, which is noted for its micrometer-scale phase separation. A clear change of resistance up to 220% was observed and the characteristic metal–insulator transition temperature T_P was also shifted. The changes of both the resistance and T_P suggest that the electric field induced not only tuning of the carrier density but also rebalancing of the phase separation states. The change of the charge-ordered insulating phase fraction was estimated to be temperature dependent, and a maximum of 16% was achieved in the phase separation regime. This tuning effect was partially irreversible, which might be due to an oxygen vacancy migration that is driven by the huge applied electric field.

Keywords: electric double-layer field effect, manganites, phase separation

PACS: 85.30.Tv, 78.30.cd, 64.75.Gh **DOI:** 10.1088/1674-1056/23/9/098501

1. Introduction

Perovskite manganites have been intensively studied in the past two decades because of their significance in fundamental physics[1–5] and prospective applications.[6–10] The interplay among charge, spin, and lattice in these compounds leads to many intriguing phenomena, such as colossal magnetoresistance (CMR)[11,12] and phase separation.[9,13] It has been well established that the carrier density plays a crucial role in determining the physical properties of these materials.[14,15] Chemical doping is the most commonly used method to tune the system carrier density.[7,16] However, chemical doping is time consuming in sample preparation and the presence of possible chemical inhomogeneity in the sample could lead to incorrect results. Furthermore, chemical doping by element substitution would generally introduce a lattice distortion due to the difference in ionic radius. Consequently, the lattice distortion could significantly change the electric transport and magnetic properties,[17] and these influences are hard to isolate from those of the carrier density tuning effect. This could be the reason why many issues in manganites are still unsettled. In contrast to chemical doping, the electric field effect provides an alternative to manipulate the system carrier density through an electric field built up by a biased gate oxide. However, the strength of the built up electric field is often limited by this gate oxide layer, which generally has a high density of defects, such as pin holes, and thus its thickness cannot be reduced at will. The relatively modest dielectric constant is another shortcoming. Therefore, in the conventional field effect experiments, the largest sheet carrier density achieved is only on the order of 10^{13} cm^{-2}, while the sheet carrier density in manganites is usually higher than 10^{14} cm^{-2}.[18] This could be the reason for the inconsistent, and sometimes controversial, tuning results that have previously been published. For example, the metal–insulator transition temperature T_P shifted considerably with the application of a static electric field in some experiments[19,20] while it remained unchanged in others.[21,22]

In recent years, the so-called electric double-layer field effect (EDL-FE) has been considered to be a promising method to manipulate the carrier density in a channel material by an enormous electric field built up through an atomic scale EDL formed at the ionic liquid (IL)/material interface. An electric field of up to 100 MV·cm^{-1} can be built and the corresponding sheet carrier density can reach 10^{15} cm^{-2}.[23] In addition, as an IL-gating structure is introduced, there will be no restriction of dielectric lattice mismatch and no breakdown within the IL electrochemical window. By employing the EDL-FE, electronic phase transitions, including superconductivity[24,25] and metal–insulator transitions,[26] have already been demonstrated. There have been a few studies on perovskite magnetites using this method, and large resistance modulations were observed. In $La_{0.8}Ca_{0.2}MnO_3$ (LCMO) films, Dhoot *et al.* have shown that the Mott metal–insulator transition could be induced; that is, the low temperature ferromagnetic metallic state was changed to the insulating state.[27] In another work on $Ce_{1-x}Ca_xMnO_3$ (CCMO)

*Project supported by the National Basic Research Program of China (Grant Nos. 2011CBA00106 and 2014CB921401) and the National Natural Science Foundation of China (Grant Nos. 11174342, 9131208, and 11374344).

†Corresponding author. E-mail: dzheng@iphy.ac.cn

© 2014 Chinese Physical Society and IOP Publishing Ltd

films,[28] Xiang *et al.* also observed the Mott metal–insulator transition when they reduced the insulating film into a metallic one and an extremely high electroresistance (120000%) was obtained. However, despite those works, more studies are needed. On the one hand, we should explore more materials in order to obtain a more comprehensive understanding on the field effect in manganites. On the other hand, there are some unsolved issues in already published works. For example, the penetrating length of the electric field was found to be much larger than expected according to the Thomas–Fermi screening.[27] Much less resistance modulation appeared in tensile strained films than that in compressive strained films.[28] It was also shown that the resistance change in both LCMO and CCMO films did not recover to the initial value when the electric field was totally removed.[27,28] Moreover, the phase separation is considered to play a crucial role in this electric field modulation of manganites. A further analysis is needed to provide more detail about how the electric field affects these coexisted phases.

In this work, we perform an EDL-FE study on ultrathin $La_{0.325}Pr_{0.3}Ca_{0.375}MnO_3$ (LPCMO) films. This system is well known for the micrometer-scale phase separation below T_p.[29,30] The phase separation, which is due to the competition between a ferromagnetic metallic (FMM) phase and a charge-ordered insulating (COI) phase, is sensitive to external perturbations. Thus, LPCMO could be a suitable system to study the evolution of the phase separation under the influence of a carrier density change. The doping level we used (Ca: 0.375) is far from the boundaries in the phase diagram,[7] so that the metal–insulator transition tuning will be gentle and gradual without any drastic modulation effects that might be hard to define.[27] In this study, a moderate and continuous modulation of the transport properties is observed. Furthermore, we find that the tuning effect is partially irreversible and the possible reasons for this phenomenon are discussed.

2. Experimental details

The perovskite LPCMO thin films were deposited on (001)-$LaAlO_3$ substrates by pulsed laser deposition (PLD). The deposition temperature was 950 °C. The energy of the laser pulses was 450 mJ, and the repetition rate was 2 Hz. During the deposition, an oxygen flow was introduced and the pressure was kept at about 60 Pa. After the deposition, the films were annealed at 540 °C for about 40 min in 1 atmosphere oxygen. The crystalline and epitaxial features of the films were examined using X-ray diffraction (XRD). The surface morphology was characterized by atomic force microscopy (AFM). X-ray reflection (XRR) measurements were carried out and the results were used for the film thickness estimation. The film characterization results are shown in Figs. 1(a)–1(c). The θ–2θ diffraction data show that the films grow along the c axis with no detectable impurity phase. The c-axis lattice constant is 0.389 nm, which is slightly larger than the bulk sample value, indicating a small compressive strain of 0.9%. The surface roughness is about 0.3 nm. Fitting of the XRR data shows that the thickness of the films we used for this paper is about 14 nm.

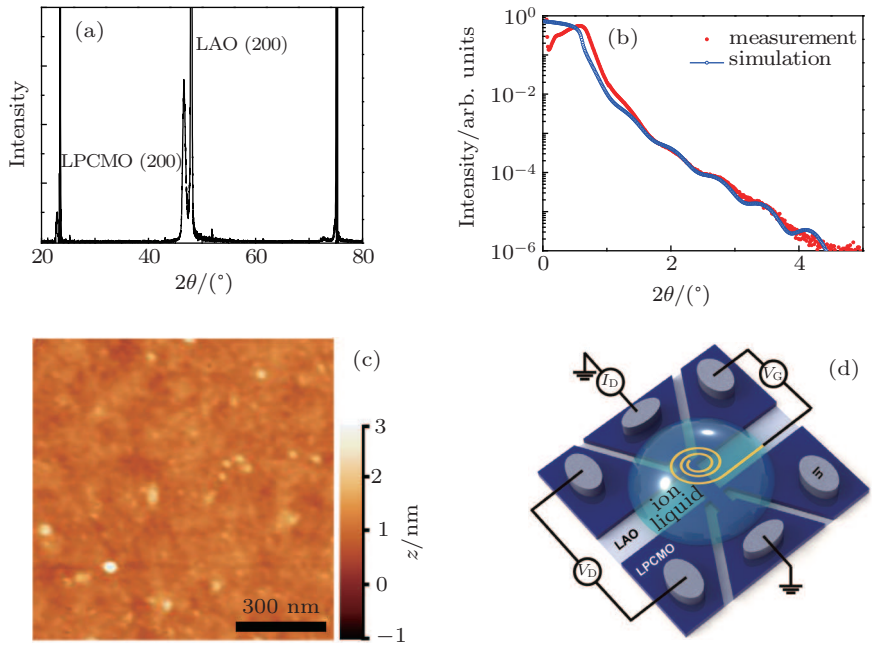


Fig. 1. (color online) Film characterizations. (a) XRD pattern, showing good crystallinity and c-axis orientation. (b) XRR spectra and the fitted curves. Simulation shows that the film thickness is about 14 nm. (c) AFM topography with a surface roughness of 0.3 nm. (d) Schematic diagram of the device pattern and the measurement circuit.

In order to carry out EDL-FE experiments, the films were patterned into a Hall bar configuration with channel sizes of 1500 μm×200 μm by ultraviolet lithography and argon-ion milling. Wire leads were attached to the electrodes using indium pieces with physical pressing. A coil wound with Au wire of 0.12 mm diameter was used as the gate electrode, which was located above the channel area. A droplet of IL N,N-diethyl-N-(2-methoxyethyl)-N-methylammonium bis-(trifluoromethanesulfonyl)-imide (DEME-TFSI) was let onto the channel area to form an Au/IL/LPCMO sandwich structure. The standard four-probe method was employed to measure the resistance with DC gate biases. The measurement circuit is shown in Fig. 1(d). In order to minimize the possible sample degeneration due to the contact with the IL, the system was quickly cooled down to 220 K. It has been shown that DEME-TFSI is less chemical active at this temperature.[31] The sample was biased at 220 K and then cooled down to 200 K, from which the resistance measurement was taken with decreasing temperature. An unbiased curve was measured prior to the gating processes. Then, the gate bias V_G was varied sequentially from 0 V to −3 V with 0.5 V step. When the $V_G = -3$ V curve was finished, we shut down the bias, warmed the system up to 220 K, and kept it at this temperature for several hours to release the ion accumulation at the IL/film interface. In our experiments, we found that the resistance did not fully recover to the initial value. The origin of this hysteresis behavior will be discussed in the next section. Because of the hysteresis, another 0 V biased curve was taken as the original one for the positive gating process, and then V_G was increased from 0 V to +3 V with 0.5 V step. A source–drain current of 10 nA was used for the measurements. The gate leakage current was monitored and found to be smaller than 0.2 nA. This ensured the reliability of our measurements. All of the measurements were carried out in a Quantum Design physical property measurement system (PPMS).

3. Results and discussion

3.1. Electric field tuning of resistance in LPCMO channel

In Fig. 2, we show the temperature dependence of the resistance measured under a series of V_G. On the unbiased curve, T_p is around 139 K, which is lower than that in 100 nm thick films (∼ 154 K). We attribute the degeneration to the strain effect induced by the lattice mismatch (−0.9%) between the film and the substrate. We suppose that the jumps near T_p appearing on the unbiased and the low-biased resistance curves are due to the percolation of FMM domains through the COI matrix in the phase separation regime. The phase separation in the LPCMO thin films was reported to be on the micrometer scale.[29] However, the percolative transport behavior is still observed in our sample with a channel width of 200 μm, which might be ascribed to the very small thickness of the film. With increasing magnitude of negative V_G, the resistance reduces gradually as more holes are doped into the film, while positive V_G does the opposite. This conforms to the carrier density tuning in a p-type semiconductor. At the same time, T_p is also modulated by the electric field as it is raised by the negative biases and reduced by the positive ones. The total shift of T_p is about 3.4 K for V_G varied from −3 V to +3 V. The shift of T_P with an applied electric field has been observed previously in researches using either conventional gates[19,32] or electrolytes.[24] However, we also notice that T_p remained unchanged in some of the other experiments.[21,22,33] As is known in the phase separation picture, as temperature decreases the FMM domains enlarge and finally percolate through the dominating COI phase, while the resistance peaks at T_p and then decreases rapidly as the temperature is further lowered. As a result, T_p is considered to be determined by the FMM/COI coexistence ratio. Therefore, the shift of T_P, as well as the modulation of the resistance with electric gating, indicates a rebalancing of this coexistence ratio. Furthermore, one may note that an extra cycle of $V_G = +3$ V induces further tuning of the resistance and T_p. The mechanism behind this will be discussed later.

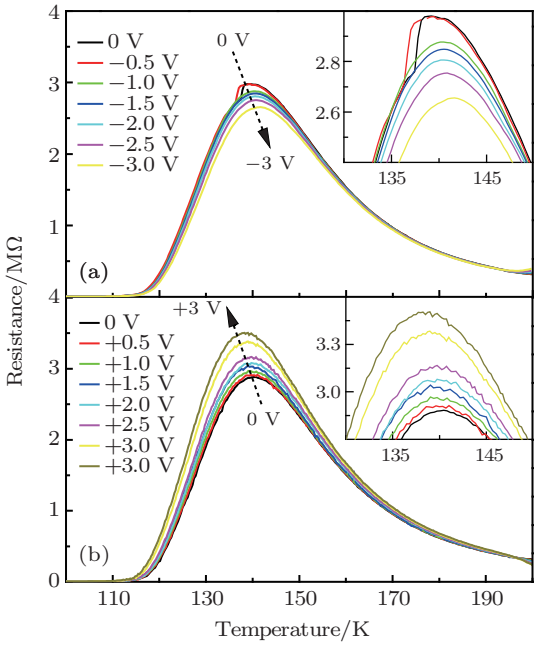


Fig. 2. (color online) The temperature dependence of the resistance measured at a series of (a) negative and (b) positive bias voltages.

The temperature dependent electroresistance (ER) was calculated at different biases, as shown in Fig. 3. With negative V_G, the ER is negative and peaks just below T_p with a maximum of −35% at $V_G = -3$ V. When positively biased, the ER is positive and follows a similar trend with temperature with a maximum of 191%. This much larger ER, which is reached by positive gating, also happened in IL-gated LCMO,[27] which

may be due to the enlarged electric field penetrating length for positive V_G when the carrier depletion happens. The total ER from -3 V to $+3$ V gating reaches 220% at about 116 K. The resistance around T_p is supposed to be sensitive to external perturbations because the coexistence of FMM and COI phases is metastable. A perturbation of carrier doping, preferring one over the other, will cause a big change in the phase balance and then in the transport properties. An extra cycle of $V_G = +3$ V induces further tuning of the resistance and T_p. Since the charging time (20 min at 220 K) is long enough for ion accumulation at the interface, this phenomenon cannot be ascribed to a boost of ions in the EDL. This indicates an effect other than the carrier accumulation that we expected and this process takes a much longer time. A similar phenomenon takes place with negative gating, but is less significant. This is most probably due to the migration of oxygen vacancies in the channel induced by the huge built-in electric field. This effect will also be discussed later.

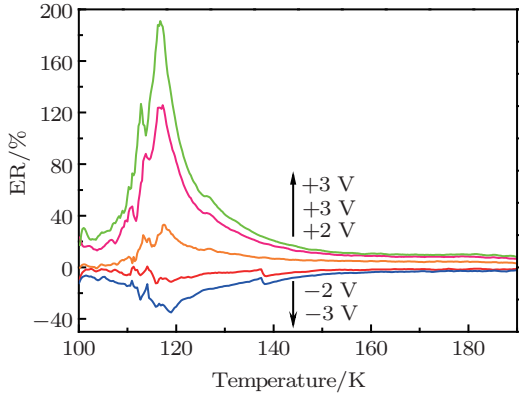


Fig. 3. (color online) The electroresistance calculated by ER = $(R_E - R_0)/R_0$, where R_E and R_0 are resistances with and without gating, respectively.

3.2. Electric field effect on high-temperature small polaronic transport

In perovskite manganites, the electric transport in the high-temperature regime is polaronic.[34–36] At temperatures above 160 K, our resistance versus temperature curve could be fitted by the small polaron model,[34] that is

$$\rho = \frac{A}{T}\exp\left[\frac{E_{hop}}{k_B T}\right],$$

where E_{hop} is the polaron activation energy, and A is a constant referring to the specific material. The fact that the resistance follows this polaronic relation well indicates that the film is of very good quality in terms of crystallinity.[36] In Fig. 4, the resistance data are plotted in a fashion of $\ln(R/T)$ versus $1/T$ at different V_G. The values of E_{hop} can be derived from the slopes of these curves in the linear high-temperature regime. According to the linear fitting, E_{hop} are 111.3 meV, 111.9 meV, and 113.3 meV for V_G of -3 V, 0 V, and $+3$ V, respectively. The value increases slightly with increasing gate voltage, from negative to positive. The E_{hop} is related to the strength of the John–Teller distortion, which restrains the mobility of the carriers. Therefore, in a simplified picture, we may relate the change of the resistance to the change of the carrier density by assuming unchanged carrier mobility. Moreover, the phase separation in this temperature regime is believed to be insignificant, and the relatively small ER, as shown in Fig. 3, results primarily from the change of the carrier density. We also note that the ER is almost unchanged at temperatures above 160 K, which implies that the change in the carrier density induced by the electric field does not vary much with temperature. An ER about 10% for V_G of $+3$ V and that of 3.5% for V_G of -3 V indicate the levels of carrier density doping here.

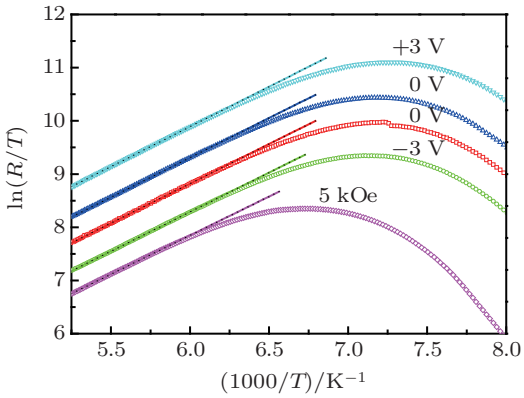


Fig. 4. (color online) $\ln(R/T)$ versus $1000/T$ with different V_G. Solid lines are linear fittings for the date in the high-temperature regime.

3.3. Correspondence of electric field and magnetic field

According to the previous work, a magnetic field could align randomly orientated Mn core spins and reinforce the FMM state in the phase separated regime.[13] This effect brings about a large magnetoresistance (MR) in manganites. To look into how this influences the phase separation during electric field gating, a magnetic field was introduced simultaneously with the electric biases. To avoid the influence of the previous measurements, another virgin sample with very similar characteristics was used here. Compared to that with no magnetic field, the ER with a magnetic field of 5 kOe was reduced significantly, especially at a temperature below T_p, as shown in Fig. 5(a). Figure 5(b) shows the MR measured at different gate voltages. It is clear that the MR is enhanced (suppressed) by a positive (negative) gating. The combined effect of magnetic field and electric field indicates that FMM/COI phase rebalancing takes place in some vulnerable regions by enlarging or reducing the FMM domains in the phase-separated regime. Since an additional magnetic field can influence these vulnerable regions and turn the COI phase into the FMM phase, a weakened ER at V_G of -3 V is reasonable. Correspondingly, with negative gating, extra carriers brought about by the electric field make the channel more conductive and the Mn core spins are aligned due to the double

exchange coupling. So, the magnetic field has less to do with the spins and produces a shrunken MR, whereas the depletion of the carriers takes place at positive V_G, more spins are left to be aligned by the magnetic field, and therefore the MR is enhanced.

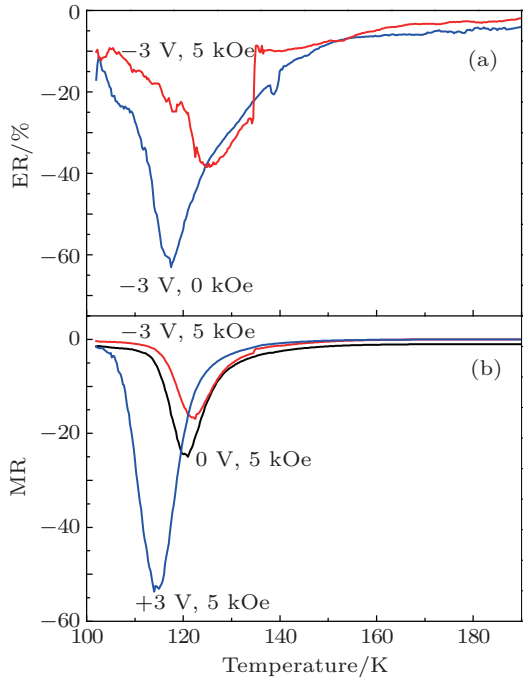


Fig. 5. (color online) (a) ER of −3 V gating with magnetic field of 0 and 5 kOe. (b) MR at 5 kOe with different V_G. Here, MR $= (R_T - R_0)/R_T$, where R_T and R_0 are resistances with and without the magnetic field, respectively.

According to the above analysis, we may draw the following picture of how the electric field influences the electric transport of this phase separated thin film. At a high temperature, the film behaves as a nominal semiconductor and the electric transport is polaronic. The carrier doping is homogeneous. As the temperature is lowered, the film moves into the FMM/COI phase separation regime, the charge accumulation or depletion would favor or suppress the formation of the FMM phase. In other words, the carrier doping becomes non-uniform. In a previous work by He *et al.* on the same material, it was shown empirically that the COI phase fraction f_{COI} measured by Lorentz transmission electron microscopy mapping followed closely the $\ln R$ obtained in the warming curve for the temperature below T_p.[30] This result provides us with a semi-quantitative way to estimate the electric field induced change in the phase fraction in LPCMO. In Fig. 6(a), we show the $\ln R$ versus $1/T$ curves for $V_G = -3$ V, 0 V, and +3 V. The star marks represent the f_{COI} obtained by comparing our results with those reported in Ref. [28]. The difference between the curves represents the change in the fraction of the COI phase. In Fig. 6(b), we plot the relative change of the COI phase fraction, Δf_{COI}, as a function of temperature. The Δf_{COI} turns out to be temperature dependent and reaches 16% at maximum. Although this estimation is rough, the result could be instructive for further studies. For instance, this amount of Δf_{COI} may cause an enhanced electric field modulation of resistance if the channel is confined to the micrometer scale, which is comparable to the phase-separated dimension in LPCMO.

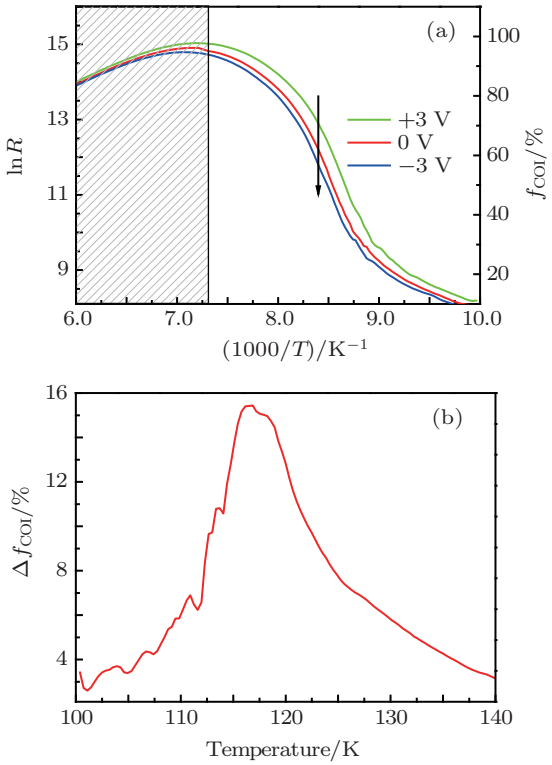


Fig. 6. (color online) (a) $\ln R$ (left axis) and estimated f_{COI} below T_p (right axis) versus $1000/T$. (b) Calculated Δf_{COI} versus temperature, where Δf_{COI} is given by $\Delta f_{COI} = (\ln R_{+3\ V} - \ln R_{-3\ V})/\ln R_0$.

3.4. Irreversibility of the electric field tuning

An unexpected effect in our electric field modulation experiments is that the resistance did not recover completely after V_G was removed and the whole device was warmed up to 220 K and held for 20 min to hours, allowing the accumulated ions to rebuild neutrality. We extract the resistance versus V_G from the resistance–temperature curve series. The hysteresis of the resistance with V_G at 150 K is shown as an example in Fig. 7. When V_G is shut down after the application of −3 V (point *d*) and +3 V (point *f*), the resistance just recovers partially. After that, another cycle of +3 V is applied and the resistance increases further (point *g*). A very slow and incomplete recovery of the resistance can be observed after a few hours waiting, as shown in the figure from point *c* to *d* and *h* to *j*. At other temperatures, the hysteresis behavior is just the same but with different values. The irreversibility has been reported in manganites[27,28] and VO_2[37] tuned by EDL-FE. However, its origin remains unclear.

One of the hypotheses is that the electrochemical reaction[38] or hydrogenation[39] at the IL/film interface happens because of the existence of impurities in the IL. To exam-

ine the possibility of existing water or other electrochemically active impurities, an I–V curve was taken along the gate–drain with V_G sweeping rate of 5 mV·s^{-1}, the result is shown in Fig. 8. The measurement was taken at 220 K, where the gating was performed. The big loop indicates a charging/discharging process with sweeping V_G. If any electrochemical reaction of impurities took place at the IL/film interface, then there should be a sudden jump in I_G when the bias exceeds a threshold. Since the I–V curve turns out to be smooth up to 3 V, we may exclude the impurity effect here. The moderate gate current is due to the charging/discharging of the anodes and cathodes in the IL for the applied V_G.

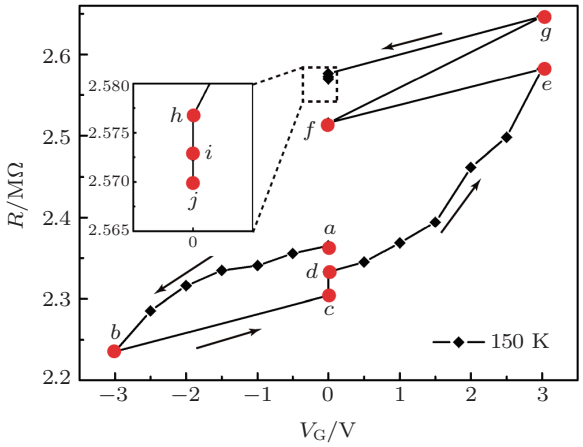


Fig. 7. Resistance hysteresis extracted from the resistance versus temperature curves at different V_G. The arrows denote the V_G variation direction.

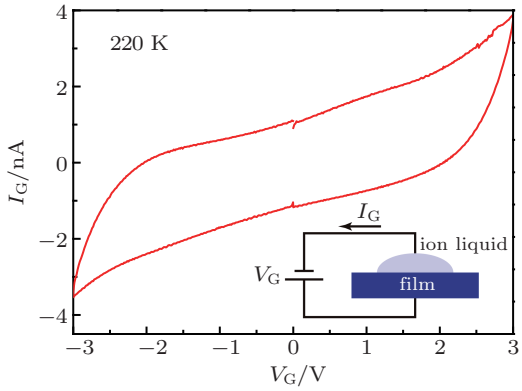


Fig. 8. (color online) The I–V characteristics of gate–drain. Inset: schematic diagram of the measurement circuit.

Taking into account the rebalancing of coexistent phases mentioned above, the pinning effect of the domain walls provides another possible cause for this irreversibility. As the phase domains enlarge or shrink, the phase boundaries may be pinned by some defects and fail to move back when the electric field is removed. Here, we figure out the contribution of such an irreversible effect, as shown in Fig. 9. It is interesting that after +3 V gating, the irreversible part mostly holds 60–70% of the total resistance modulation throughout the whole temperature range while after a −3 V bias this proportion is more dispersed. However, both curves share the trend of monotonic decrease as temperature lowers. If domain pinning acts as the main mechanism, then the irreversibility in the phase separation regime would be much stronger than that at temperature above 160 K because in this region most FMM/COI domains have melted into the paramagnetic matrix. So, it seems that domain pinning is an unlikely scenario here.

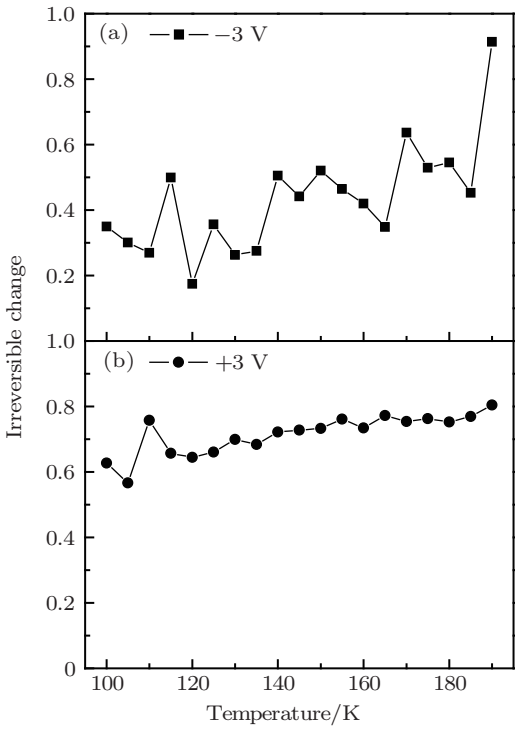


Fig. 9. Calculated irreversible part of the electric field induced resistance change. Irreversible change is calculated by $(R_c - R_a)/(R_b - R_a)$ for −3 V (a) and $(R_f - R_d)/(R_e - R_d)$ for +3 V (b). The indexes a–f are according to the points in Fig. 7.

Another possibility comes from the relocation of doping centers (Ca^{2+}, Pr^{3+}, or oxygen vacancies). Along with the charge accumulation, a huge built-in field induced by the external electric field may drag these doping centers away from their balanced positions. Such cation or vacancy displacements and relaxations are supposed to be slow and they are sometimes incomplete. This phenomenon conforms to the observed partial irreversibility in our device. Compared to the displacement of cations, the oxygen vacancy movement seems easier and may cause a sluggish irreversible resistance change and gradual recovery. This oxygen vacancy relocation has been discussed in electric field induced resistance switching in perovskite STO[40] and manganites.[41]

4. Conclusion

We have carried out an experimental study on the effect of an electric field on the transport properties of LPCMO thin films using an ionic-liquid gated EDL-FE structure. A large resistance modulation of up to 220% with relatively small gate voltages (V_G up to ±3 V) was observed in the temperature

around the metal–insulator transition temperature T_P, where the strong phase separation was present. Such a modulation can be attributed to electric field induced carrier doping, as well as rebalancing of coexisting FMM/COI phases. By using negative (positive) gating, the electric field enlarged (reduced) the FMM domains in the phase separation regime. The change of the COI phase fraction, Δf_{COI}, was temperature dependent and reached a maximum value of 16%. The strong electric field also introduced an irreversible effect, especially at positive biases, which were maintained for a long time after the external electric field was totally removed. Compared to other possible mechanisms, in this case the built-in electric field induced migration of oxygen vacancies in the channel is taken to be a possible reason. This effect should be considered in further research in doped oxides.

References

[1] Moreo A, Yunoki S and Dagotto E 1999 *Science* **283** 2034
[2] Prellier W, Lecoeur P and Mercey B 2001 *J. Phys.: Condens. Matter* **13** R915
[3] Dagotto E, Hotta T and Moreo A 2001 *Physics Reports* **344** 1
[4] Kim K, Uehara M, Hess C, Sharma P and Cheong S 2000 *Phys. Rev. Lett.* **84** 2961
[5] Siwach P, Singh H and Srivastava O 2008 *J. Phys.: Condens. Matter* **20** 273201
[6] Jin S, Tiefel T H, McCormack M, Fastnacht R A, Ramesh R and Chen L H 1994 *Science* **264** 413
[7] Schiffer P, Ramirez A, Bao W and Cheong S 1995 *Phys. Rev. Lett.* **75** 3336
[8] Mathews S 1997 *Science* **276** 238
[9] Uehara M, Mori S, Chen C H and Cheong S W 1999 *Nature* **399** 560
[10] Guo H, Noh J H, Dong S, Rack P D, Gai Z, Xu X, Dagotto E, Shen J and Ward T Z 2013 *Nano Lett.* **13** 3749
[11] Jin S, Tiefel T H, McCormack M, Fastnacht R, Ramesh R and Chen L 1994 *Science* **264** 413
[12] Anane A, Renard J P, Reversat L, Dupas C, Veillet P, Viret M, Pinsard L and Revcolevschi A 1999 *Phys. Rev. B* **59** 77
[13] Fäth M, Freisem S, Menovsky A, Tomioka Y, Aarts J and Mydosh J 1999 *Science* **285** 1540
[14] Zou L J 2001 *Phys. Rev. B* **63** 155103
[15] Alexandrov A and Bratkovsky A 1999 *Phys. Rev. Lett.* **82** 141
[16] Moritomo Y, Asamitsu A, Kuwahara H and Tokura Y 1996 *Nature* **380** 141
[17] Hwang H, Cheong S W, Radaelli P, Marezio M and Batlogg B 1995 *Phys. Rev. Lett.* **75** 914
[18] Ahn C, Triscone J M and Mannhart J 2003 *Nature* **424** 1015
[19] Pallecchi I, Pellegrino L, Bellingeri E, Siri A, Marré D, Tebano A and Balestrino G 2008 *Phys. Rev. B* **78** 024411
[20] Liao J H, Wu T B, Chen Y T and Wu J M 2007 *J. Appl. Phys.* **101** 09M110
[21] Wu T, Ogale S, Garrison J, Nagaraj B, Biswas A, Chen Z, Greene R, Ramesh R, Venkatesan T and Millis A 2001 *Phys. Rev. Lett.* **86** 5998
[22] Hu F X and Gao J 2006 *Appl. Phys. Lett.* **88** 132502
[23] Ueno K, Nakamura S, Shimotani H, Ohtomo A, Kimura N, Nojima T, Aoki H, Iwasa Y and Kawasaki M 2008 *Nat. Mater.* **7** 855
[24] Ye J T, Inoue S, Kobayashi K, Kasahara Y, Yuan H T, Shimotani H and Iwasa Y 2010 *Nat. Mater.* **9** 125
[25] Bollinger A T, Dubuis G, Yoon J, Pavuna D, Misewich J and Bozovic I 2011 *Nature* **472** 458
[26] Jeong J, Aetukuri N, Graf T, Schladt T D, Samant M G and Parkin S S 2013 *Science* **339** 1402
[27] Dhoot A, Israel C, Moya X, Mathur N and Friend R 2009 *Phys. Rev. Lett.* **102** 136402
[28] Xiang P H, Asanuma S, Yamada H, Inoue I H, Sato H, Akoh H, Sawa A, Ueno K, Yuan H, Shimotani H, Kawasaki M and Iwasa Y 2011 *Adv. Mater.* **23** 5822
[29] Zhang L, Israel C, Biswas A, Greene R L and de Lozanne A 2002 *Science* **298** 805
[30] He J, Volkov V, Asaka T, Chaudhuri S, Budhani R and Zhu Y 2010 *Phys. Rev. B* **82** 224404
[31] Yuan H, Shimotani H, Ye J, Yoon S, Aliah H, Tsukazaki A, Kawasaki M and Iwasa Y 2010 *J. Am. Chem. Soc.* **132** 18402
[32] Pandey N, Lobo R and Budhani R 2003 *Phys. Rev. B* **67** 054413
[33] Hu F X and Gao J 2006 *J. Appl. Phys.* **99** 08Q314
[34] Jaime M, Salamon M B, Rubinstein M, Treece R E, Horwitz J S and Chrisey D B 1996 *Phys. Rev. B* **54** 11914
[35] Jaime M, Hardner H, Salamon M, Rubinstein M, Dorsey P and Emin D 1997 *Phys. Rev. Lett.* **78** 951
[36] Ziese M and Srinitiwarawong C 1998 *Phys. Rev. B* **58** 11519
[37] Nakano M, Shibuya K, Okuyama D, Hatano T, Ono S, Kawasaki M, Iwasa Y and Tokura Y 2012 *Nature* **487** 459
[38] Zhou Y and Ramanathan S 2012 *J. Appl. Phys.* **111** 084508
[39] Yuan H, Shimotani H, Tsukazaki A, Ohtomo A, Kawasaki M and Iwasa Y 2010 *J. Am. Chem. Soc.* **132** 6672
[40] Szot K, Speier W, Bihlmayer G and Waser R 2006 *Nat. Mater.* **5** 312
[41] Quintero M, Levy P, Leyva A and Rozenberg M 2007 *Phys. Rev. Lett.* **98** 116601